

Landé-like formula for the g factors of hole-nanowire subband edges

D. Csontos and U. Zülicke

*Institute of Fundamental Sciences and MacDiarmid Institute for Advanced Materials and Nanotechnology,
Massey University, Private Bag 11 222, Palmerston North 4442, New Zealand*

P. Brusheim and H. Q. Xu

Division of Solid State Physics, Lund University, Box 118, S-22100 Lund, Sweden

(Dated: June 21, 2024)

We have analyzed theoretically the Zeeman splitting of hole-quantum-wire subband edges. As is typical for any bound state, their g factor depends on both a vacuum (here: bulk-material) g factor and an additional contribution arising from a finite bound-state orbital angular momentum. We discuss the quantum-confinement-induced interplay between bulk-material and orbital effects, which is nontrivial due to the presence of strong spin-orbit coupling. A compact analytical formula is provided that elucidates this interplay and can be useful for predicting Zeeman splitting in generic hole-wire geometries.

The interaction of a particle's magnetic moment with an external magnetic field \mathbf{B} typically results in the lifting of degeneracies in its energy spectrum. The study of such Zeeman splittings provides important clues about microscopic properties of a quantum system.¹ In vacuum or the bulk of a solid, the Zeeman splitting can be understood as arising from the coupling of a (quasi-)free particle's intrinsic angular momentum (i.e., spin) to \mathbf{B} . However, in general, orbital motion in a quantum bound state is associated with a magnetic moment that interacts with the magnetic field and, thus, also contributes to Zeeman splitting and the g factor. In the presence of spin-orbit coupling, the interplay between orbital and intrinsic (spin) contributions to g can be nontrivial.¹

Recently, p -type semiconductor nanostructures have become available as interesting laboratories to explore the interplay between quantum confinement and the magnetic moment of spin-3/2 holes.^{2,3,4,5,6,7,8,9} For example, strong spin-orbit coupling present in the upper-most valence band of typical semiconductors results in an energy splitting¹⁰ between heavy-hole (HH) and light-hole (LH) quantum-well subband edges.¹¹ This HH-LH splitting turns out to freeze the HH spin-projection axis to be perpendicular to the quantum well, thus preventing its reorientation by an in-plane magnetic field and, therefore, suppressing Zeeman splitting.^{2,12} In addition to HH-LH *splitting*, confinement typically induces a *mixing* of HH and LH states in quantum wires,^{13,14,15,16} even at subband edges. Both HH-LH mixing and splitting strongly affect the physical properties of hole states.

We have previously shown^{15,17} how HH-LH mixing modifies the Zeeman splitting of hole-wire subband-edges when the bulk-material hole g factor κ is large and can be assumed to dominate over all orbital magnetic-field effects.¹⁸ Here we complement this analysis of Zeeman splitting in hole quantum wires, focusing on the confinement-induced interplay between bulk-material and orbital bound-state contributions to the g factor. Bulk-material and orbital contributions turn out to vary strongly between different quantum-wire subband edges, in both their magnitude and sign. Depending on their relative sign, the two contributions can either enhance or suppress each other, thus yielding large variations in sign and magnitude of the total g factor. We provide a formula from which the origins of the observed spin-splitting characteristics can

be explained and which may also be useful to predict Zeeman splittings in generic hole-wire geometries. For cylindrical hole wires, we also find a Landé-like formula, which explicitly expresses the subband-edge g factor in terms of a new total angular momentum and spin-3/2 tensor invariants,¹⁹ the latter resulting from a multipole expansion of the spin-3/2 density matrix. It is an interesting feature of spin-3/2 systems that, in addition to a monopole and dipole moment, which are related to the density and polarization, respectively, a quadrupole and an octupole moment can exist, which have no equivalents in spin-1/2 systems. Orbital contributions turn out to give rise to a dependence of the hole-wire g factors on spin-3/2 quadrupole and octupole moments.

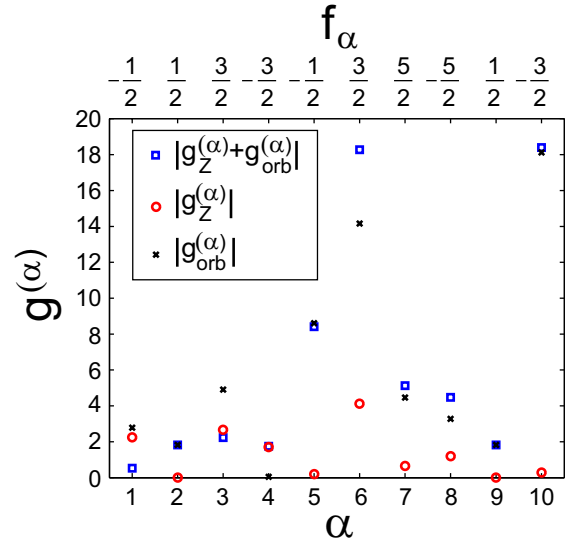


FIG. 1: (Color online) Absolute values of orbital and bulk-material Zeeman contributions, $g_{orb}^{(\alpha)}$ and $g_Z^{(\alpha)}$, to the total g -factor, $g_{tot}^{(\alpha)} = g_Z^{(\alpha)} + g_{orb}^{(\alpha)}$, for a cylindrical hole nanowire defined by a hard-wall confinement in GaAs (i.e., a material with Luttinger parameters $\gamma_1 = 6.98$, $\gamma_s = 2.58$, and $\kappa = 1.2$; see text). Values are shown for the highest-in-energy subband edges enumerated by α . f_α is the quantum number of the total angular momentum operator $\hat{F}_z = \hat{J}_z + \hat{L}_z$. The magnetic field is assumed to be parallel to the wire (z) axis.

TABLE I: g -factor contributions for cylindrical-hole-nanowire subband edges in GaAs, with cubic corrections neglected.

α, f_α	1, $-\frac{1}{2}$	2, $\frac{1}{2}$	3, $\frac{3}{2}$	4, $-\frac{3}{2}$	5, $-\frac{1}{2}$	6, $\frac{3}{2}$	7, $\frac{5}{2}$	8, $-\frac{5}{2}$	9, $\frac{1}{2}$	10, $-\frac{3}{2}$
$g_{\text{tot}}^{(\alpha)}$	-0.52	-1.82	2.23	1.75	8.44	-18.23	-5.12	4.48	-1.82	18.34
$g_Z^{(\alpha)}$	2.26	0.00	-2.68	1.70	-0.19	-4.12	-0.66	1.20	0.00	0.28
$g_{\text{orb,diag}}^{(\alpha)}$	0.55	-1.82	-8.27	12.30	10.32	-5.66	-24.1	24.9	-1.82	19.5
$g_{\text{orb,mix}}^{(\alpha)}$	-3.33	0.00	13.18	-12.25	-1.69	-8.45	19.64	-21.62	0.00	-1.44

Figure 1 shows our calculated absolute values of bulk-material and orbital contributions $|g_Z^{(\alpha)}|$, $|g_{\text{orb}}^{(\alpha)}|$ to the total g -factor $|g_{\text{tot}}^{(\alpha)}| = |g_Z^{(\alpha)} + g_{\text{orb}}^{(\alpha)}|$, respectively, for cylindrical-hole-wire subband edges. The integer α enumerates wire subbands, starting with the highest. The magnetic field is assumed to be applied parallel to the wire, which is aligned with the z -coordinate axis, and we used materials parameters characteristic for GaAs²⁰ but with band warping neglected. Several observations can be made. i) The orbital contributions generally have a magnitude of the same order as that of the corresponding bulk-material ones. In some instances, such as for levels $\alpha = 5, 6$ and 10, they greatly exceed the bulk-material contributions, giving rise to very large spin splittings. ii) The bulk-material and orbital contributions fluctuate in sign and magnitude between different subbands. iii) The two contributions can variably enhance or suppress each other, thus rendering large variations in sign and magnitude of the total g -factor $g_{\text{tot}}^{(\alpha)}$ as a function of subband index α . Further below we discuss how the observed behavior results from HH-LH mixing.

Before describing details of our calculational method and giving further results, we discuss the general form of the various g -factor contributions. As the hole-wire subband edges are well-separated in energy, it is possible to calculate their Zeeman splitting analytically within a perturbative approach that becomes exact in the limit of $\mathbf{B} \equiv B_z \hat{\mathbf{z}} \rightarrow \mathbf{0}$. We find the following general expression $g_{\text{tot}}^{(\alpha)} = g_Z^{(\alpha)} + g_{\text{orb,diag}}^{(\alpha)} + g_{\text{orb,mix}}^{(\alpha)} + g_{\text{orb,cub}}^{(\alpha)}$. The first three terms are independent of the wire's direction with respect to crystallographic axes, neglect band warping and have the following form:

$$g_Z^{(\alpha)} = -4\kappa \langle \hat{J}_z \rangle_\alpha, \quad (1a)$$

$$g_{\text{orb,diag}}^{(\alpha)} = -2\gamma_1 \langle \hat{L}_z \mathbb{1}_{4 \times 4} \rangle_\alpha - 2\gamma_s \left\langle \left(\hat{J}_z^2 - \frac{5}{4} \mathbb{1}_{4 \times 4} \right) \hat{L}_z \right\rangle_\alpha, \quad (1b)$$

$$g_{\text{orb,mix}}^{(\alpha)} = -2\gamma_s \left\langle i\hat{x} - \hat{k}_- \hat{J}_+^2 - i\hat{x} + \hat{k}_+ \hat{J}_-^2 \right\rangle_\alpha. \quad (1c)$$

Here $\langle \dots \rangle_\alpha$ denotes the expectation value of the operator inside the angular brackets taken for the positive-helicity eigenstate^{14,21} of wire subband edge α obtained in zero magnetic field. κ is the bulk-hole g -factor,²² $\hat{L}_z = x\hat{k}_y - y\hat{k}_x$, $\hat{x}_\pm = x \pm iy$, $\hat{k}_\pm = \hat{k}_x \pm i\hat{k}_y$, $\hat{J}_\pm = (\hat{J}_x \pm i\hat{J}_y)/\sqrt{2}$, \hat{k}_i are orbital linear momenta, \hat{J}_i are spin-3/2 angular-momentum operators, and $\gamma_s = (2\gamma_2 + 3\gamma_3)/5$ in terms of Luttinger parameters.^{22,23}

The band-warping correction $g_{\text{orb,cub}}^{(\alpha)}$ depends on the wire direction.²⁴ For now, we continue neglecting this term in our

calculations, postponing a discussion of its effect on our results to the end of the paper.

As previously discussed, it is a general characteristic of hole nanowire subband edges that they are mixtures of HH and LH characters.^{13,14,15} Thus, all of the individual terms in the expression of $g_{\text{tot}}^{(\alpha)}$ are affected by HH-LH mixing, because the expectation value is taken with respect to a HH-LH mixed nanowire subband-edge state. It was previously shown that the bulk-material contribution $g_Z^{(\alpha)}$ fluctuates strongly between different subband edges as a result thereof.^{15,17}

The orbital contributions $g_{\text{orb,diag}}^{(\alpha)}$ and $g_{\text{orb,mix}}^{(\alpha)}$ show similar behaviour, as can be seen from their values given in Table I. Interestingly, with only few exceptions (e.g., the level with $\alpha = 6$), these two terms appear to counteract each other, sometimes quite dramatically. (See e.g., levels with $\alpha = 4$ and 8.) $g_{\text{orb,diag}}^{(\alpha)}$ has a straightforward interpretation in that it represents the naïve coupling of a bound-state orbital magnetic moment to the external magnetic field, with different gyromagnetic ratio for HH and LH states because of their different effective masses. The term $g_{\text{orb,mix}}^{(\alpha)}$ arises because the spin-orbit coupling in the valence band induces linear-in- B terms that couple HH and LH amplitudes directly. Thus it represents a HH-LH mixing effect on top of the mixing already present in the spin-3/2 subband-edge states.

The total g factor $g_{\text{tot}}^{(\alpha)}$ is a sum of bulk-material and orbital terms. As seen in Table I, these different terms can vary substantially in magnitude and sign between different subband edges α as a result of the HH-LH mixing. More importantly, the relative sign between the various contributions is different between the subband edges. Thus, the bulk-material and orbital terms can variably enhance or suppress each other's contribution to the total g factor depending on the subband index α .

We now proceed to discussing in detail the theoretical formalism for calculating the total g -factor and its individual contributions given in Eqs. (1a)–(1c). Subsequently, we will show that their basic characteristics discussed above are universal for quasi-1D hole systems by considering the influence of reduced symmetry of the confining potential. We will also analyze the effect of (so far neglected) cubic corrections.

Our starting point is the Luttinger Hamiltonian²² in the spherical approximation²³

$$H_L = -\frac{\gamma_1}{2} \hat{k}^2 \mathbb{1}_{4 \times 4} + \gamma_s \left[(\hat{\mathbf{k}} \cdot \hat{\mathbf{J}})^2 - \frac{5}{4} \hat{k}^2 \mathbb{1}_{4 \times 4} \right]. \quad (2)$$

In Eq. (2), we used atomic units. In the following, we assume $\hat{k}_z = 0$ because we will focus solely on the properties

of quasi-1D subband edges. The bulk-hole Zeeman interaction with a magnetic field applied along the wire (z) direction is given by $H_Z = -2\kappa\mu_B B_z \hat{J}_z$. (We neglect the small anisotropic part¹² of the Zeeman splitting in the bulk valence band.) This term is the origin of the contribution $g_Z^{(\alpha)}$ to the hole-wire g factor. The orbital effect of the magnetic field is included by replacing $\hat{\mathbf{k}} \rightarrow \hat{\mathbf{k}} + \mathbf{A}$, with the symmetric gauge

$\mathbf{A} = (-y/2, x/2, 0)B_z$. As we will only consider the leading (linear-in- B_z) contribution to the Zeeman splitting, we neglect orbital terms of higher than linear order in B_z . The additional Hamiltonian, H_{orb} , which incorporates the effects due to the interaction between the holes' orbital degrees of freedom and the magnetic field, is then given by

$$H_{\text{orb}} = -\mu_B B_z \left\{ \left[\gamma_1 \mathbb{1}_{4 \times 4} + \gamma_s \left(\hat{J}_z^2 - \frac{5}{4} \mathbb{1}_{4 \times 4} \right) \right] \hat{L}_z + i\gamma_s \left(\hat{x}_- \hat{k}_- \hat{J}_+^2 - \hat{x}_+ \hat{k}_+ \hat{J}_-^2 \right) \right\}. \quad (3)$$

The first term, proportional to \hat{L}_z and diagonal in spin-3/2 space, gives rise to the diagonal orbital contribution $g_{\text{orb,diag}}^{(\alpha)}$. The second term couples HH and LH states and leads to $g_{\text{orb,mix}}^{(\alpha)}$.

For $\hat{k}_z = 0$, the Hamiltonian $H_B = H_L + H_Z + H_{\text{orb}}$ turns out to be block-diagonal in spin-3/2 space such that subspaces for helicity \pm do not couple.^{14,21} Subband energies $E_{\alpha\pm}$ within the \pm subspaces are found by diagonalising corresponding blocks in $H_B + V(x, y)$, where $V(x, y)$ is the confining potential defining the wire. For any given α , eigenstates $|\alpha\pm\rangle$ with energies $E_{\alpha\pm}$ are found to be degenerate at zero magnetic field, but these split for $B_z > 0$. We define the g factor for a hole-wire subband edge with index α according to $g_{\text{tot}}^{(\alpha)} = \lim_{B_z \rightarrow 0} [E_{\alpha+}(B_z) - E_{\alpha-}(B_z)] / (\mu_B B_z)$. Because of the finite energy separation of subband edges for different α , this definition turns out to be equivalent to the perturbative (to first order in B_z) result

$$\begin{aligned} g_{\text{tot}}^{(\alpha)} &= \frac{\langle H_Z + H_{\text{orb}} \rangle_{\alpha+} - \langle H_Z + H_{\text{orb}} \rangle_{\alpha-}}{\mu_B B_z} \\ &\equiv \frac{2\langle H_Z + H_{\text{orb}} \rangle_{\alpha+}}{\mu_B B_z}, \end{aligned} \quad (4)$$

where the expectation values are taken with respect to the wire eigenstates that diagonalize the zero-field, quantum-confined Luttinger Hamiltonian $H_L + V(x, y)$.

An interesting case arises for hole wires with cylindrical cross-section. There, subband-edge bound states are also eigenstates of a new total angular momentum $\hat{F}_z \equiv \hat{J}_z + \hat{L}_z$.^{14,15,17} This makes it possible to rewrite Eqs. (1) in terms of the quantum number f_α associated with \hat{F}_z , as well as expectation values of spin-3/2 operators, thereby essentially eliminating any dependence on the orbital angular momentum \hat{L}_z .

In the spherical approximation, we find $g_{\text{tot,cyl}}^{(\alpha)} = g_{\text{d,cyl}}^{(\alpha)} +$

$g_{\text{o,cyl}}^{(\alpha)} + g_{\text{r,cyl}}^{(\alpha)}$, where

$$g_{\text{d,cyl}}^{(\alpha)} = -2\gamma_1 f_\alpha - (4\kappa - 2\gamma_1) \langle \hat{J}_z \rangle_\alpha, \quad (5a)$$

$$g_{\text{q,cyl}}^{(\alpha)} = -2\gamma_s f_\alpha \left\langle \hat{J}_z^2 - \frac{5}{4} \mathbb{1}_{4 \times 4} + \hat{J}_+^2 + \hat{J}_-^2 \right\rangle_\alpha, \quad (5b)$$

$$g_{\text{o,cyl}}^{(\alpha)} = 2\gamma_s \left\langle \left[\hat{J}_z^2 - \frac{5}{4} \mathbb{1}_{4 \times 4} + \hat{J}_+^2 + \hat{J}_-^2 \right] \hat{J}_z \right\rangle_\alpha, \quad (5c)$$

$$g_{\text{r,cyl}}^{(\alpha)} = -2\gamma_s \left\langle \left[\hat{J}_+^2 - \hat{J}_-^2 \right] r \partial_r \right\rangle_\alpha. \quad (5d)$$

Here r is the radial coordinate in the xy plane, and expectation values are to be taken in the radial spinor wave functions that are eigenfunctions of the canonically transformed Hamiltonian $e^{i\hat{J}_z\varphi} [H_L + V(r)] e^{-i\hat{J}_z\varphi}$.¹⁵

In Eqs. (5a-c), expectation values are taken of spherical tensor operators associated with multipole invariants of the spin-3/2 density matrix.¹⁹ The contribution $g_{\text{d,cyl}}$ depends on the dipole moment, or polarization, of the hole-wire bound state. It contains the previously analyzed^{15,17} bulk-material contribution that is proportional to κ . Interestingly, expectation values of tensor components for spin-3/2 quadrupole and octupole moments appear in the additional terms $g_{\text{q,cyl}}$ and $g_{\text{o,cyl}}$, respectively. Such quadrupole and octupole moments are a unique feature of spin-3/2 systems and have no equivalent in the spin-1/2 realm. Situations can arise in which the dipole moment (polarization) is very small, but higher moments can be substantial. For example, a magnetic field applied parallel to a two-dimensional hole system can induce a large octupole moment, whilst the dipole moment associated with the polarization is vanishing.¹⁹ For the hole nanowires, the appearance of higher moments in the g factor are entirely due to orbital effects, which is signified by their dependence on the Luttinger parameters. The remainder term $g_{\text{r,cyl}}$ is of purely orbital origin but does not appear to have a straightforward relation to pure spin-3/2 tensors.

To verify the validity of our approximations and the use of the perturbation approach, we have performed calculations taking into account the effects of lower symmetries of the confining potential, as well as the underlying crystal, and compared these results with numerical diagonalization of the full Luttinger Hamiltonian including band warping^{22,23,24}. Our re-

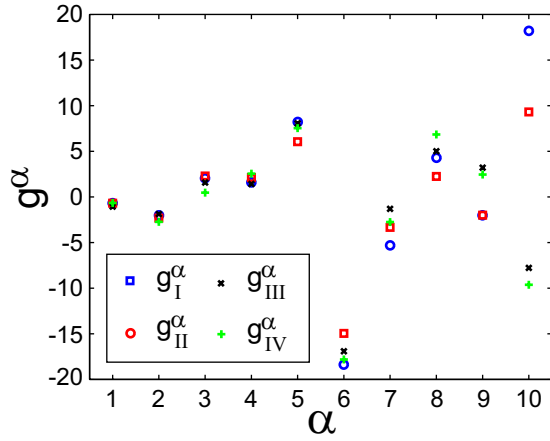


FIG. 2: (Color online) Total g -factors for hole wire subband edges labelled by index $\alpha = 1 \dots 10$, calculated using a hierarchy of approximations described in the text. A close agreement between the different results for low-index subbands is observed, while corresponding numbers show an increasing spread for higher-index subband edges.

sults are shown in Fig. 2, where we plot the total g -factors for the ten highest wire subband edges with index $\alpha = 1 \dots 10$, calculated using a hierarchy of four different approximations: **I** Perturbation theory for $H_{\text{orb}} + H_Z$ using unperturbed states that diagonalize the Hamiltonian $H_L + V(x, y)$ for a cylindrical hard-wall potential. (These are the same results as shown in Fig. 1 and Table I). **II** Same as **I**, except that the wire is defined by a hard-wall potential with *square* crosssection, thus reducing the symmetry of the confining potential. **III** Same as **II**, but the unperturbed states are obtained by diagonalizing the zero-field Luttinger Hamiltonian including band-warping

terms, thus taking into account the lower (cubic) crystal symmetry.²² (For this case, the wire is assumed to be parallel to the [001] direction.) **IV** Results obtained from full numerical diagonalization of the Luttinger Hamiltonian with finite magnetic field, including band warping, for a square cross-section wire parallel to the [001] direction.²⁴ Comparison between these different cases shows good agreement for states with low subband index α . For higher α , however, the effects of reduced symmetry are more pronounced, and there appears an increased spread between the g -factors calculated for different approximations. We expect that these will become even more important for wires aligned with crystallographic directions other than the high-symmetry [001] direction considered in our calculations.

In conclusion, we have presented a comprehensive and general formalism for the description of the Zeeman splitting of hole-quantum-wire subband edges and applied it to hole wires subject to a magnetic field applied parallel to the wire axis. We have elucidated the role of HH-LH mixing in hole nanowire systems, as well as the intricate quantum-confinement-induced interplay between the bulk-material and orbital contributions to the total g factors. The latter may be used for tailoring of hole spin splittings by tuning the relative importance of the two contributions, e.g., by electrostatic confinement engineering in p -type quantum point contacts²⁵ or nanowires.⁵

DC acknowledges partial support from the Massey University Research Fund and thanks the Division of Solid State Physics/Nanometer Structure Consortium, Lund University, Sweden, for their hospitality, and the Swedish Research Council (VR) for financial support during the part of the work that was completed in Sweden.

- ¹ J. H. van Vleck, *The Theory of Electric and Magnetic Susceptibilities* (Oxford U Press, London, 1932).
- ² R. Winkler, S. J. Papadakis, E. P. De Poortere, and M. Shayegan, *Phys. Rev. Lett.* **85**, 4574 (2000).
- ³ K.-M. Haendel, R. Winkler, U. Denker, O. G. Schmidt, and R. J. Haug, *Phys. Rev. Lett.* **96**, 086403 (2006).
- ⁴ R. Danneau et al., *Phys. Rev. Lett.* **97**, 026403 (2006).
- ⁵ H.-Y. Li et al., *Nano Lett.* **7**, 1144 (2007).
- ⁶ C. E. Pryor and M. E. Flatté, *Phys. Rev. Lett.* **96**, 026804 (2006).
- ⁷ A. De and C. E. Pryor, *Phys. Rev. B* **76**, 155321 (2007).
- ⁸ W. Sheng and A. Babinski, *Phys. Rev. B* **75**, 033316 (2007).
- ⁹ X.-W. Zhang, W.-J. Fan, K. Chang, S.-S. Li, and J.-B. Xia, *Appl. Phys. Lett.* **91**, 113108 (2007).
- ¹⁰ E. I. Rashba and E. Y. Sherman, *Phys. Lett. A* **129**, 175 (1988).
- ¹¹ HH and LH states are spin-3/2-projection eigenstates with eigenvalues $\pm 3/2$ and $\pm 1/2$, respectively.
- ¹² R. Winkler, *Spin-Orbit Coupling Effects in Two-Dimensional Electron and Hole Systems* (Springer, Berlin, 2003).
- ¹³ G. Bastard, J. A. Brum, and R. Ferreira, *Solid State Physics* (Academic Press, San Diego, 1991), vol. 44, pp. 229–415.
- ¹⁴ P. C. Sercel and K. J. Vahala, *Phys. Rev. B* **42**, 3690 (1990).
- ¹⁵ D. Csontos and U. Zülicke, *Phys. Rev. B* **76**, 073313 (2007).
- ¹⁶ Q. Zhu, K. F. Karlsson, E. Pelucchi, and E. Kapon, *Nano Lett.* **7**,

2227 (2007).

- ¹⁷ D. Csontos and U. Zülicke, *Appl. Phys. Lett.* **92**, 023108 (2008).
- ¹⁸ This approach applies in dilute magnetic hole wires²⁶ where the bulk-hole g factor is enhanced by a p - d exchange mechanism.²⁷
- ¹⁹ R. Winkler, *Phys. Rev. B* **70**, 125301 (2004).
- ²⁰ I. Vurgaftman, J. R. Meyer, and L. R. Ram-Mohan, *J. Appl. Phys.* **89**, 5815 (2001).
- ²¹ Helicity \pm distinguishes the two subspaces spanned by \hat{J}_z eigenstates with quantum numbers $\{\pm 3/2, \mp 1/2\}$, respectively.
- ²² J. M. Luttinger, *Phys. Rev.* **102**, 1030 (1956).
- ²³ N. O. Lipari and A. Baldereschi, *Phys. Rev. Lett.* **25**, 1660 (1970).
- ²⁴ The cubic-symmetry term that accounts for band-warping effects depends on the wire's direction with respect to crystallographic axes.²² For a wire oriented parallel to the [001] direction, it reads
$$g_{\text{orb,cub}}^{(\alpha)} = -\frac{\gamma_2 - \gamma_3}{20} \left[12 \left\langle \left(\hat{J}_z^2 - \frac{5}{4} \mathbb{1}_{4 \times 4} \right) \hat{L}_z \right\rangle_{\alpha} - 5 \left\langle i\hat{x} + \hat{k}_+ \hat{J}_+^2 - i\hat{x} - \hat{k}_- \hat{J}_-^2 \right\rangle_{\alpha} - \left\langle i\hat{x} + \hat{k}_+ \hat{J}_-^2 - i\hat{x} - \hat{k}_- \hat{J}_+^2 \right\rangle_{\alpha} \right].$$
- ²⁵ O. Klochan et al., *Appl. Phys. Lett.* **89**, 092105 (2006).
- ²⁶ F. Martelli et al., *Nano Lett.* **6**, 2130 (2006).
- ²⁷ T. Dietl, H. Ohno, and F. Matsukura, *Phys. Rev. B* **63**, 195205 (2001).